

Effect of Biosynthesized Zinc oxide Nanoparticles on Phenotypic and Genotypic Biofilm Formation of *Proteus mirabilis*

Noor Hamza Faiq *, Mais E. Ahmed 

Department of Biology, Collage of Science, University of Baghdad, Baghdad, Iraq.

*Corresponding Author.

Received 07/11/2022, Revised 25/02/2023, Accepted 27/02/2023, Published Online First 20/08/2023,
Published 01/03/2024



© 2022 The Author(s). Published by College of Science for Women, University of Baghdad. This is an Open Access article distributed under the terms of the [Creative Commons Attribution 4.0 International License](https://creativecommons.org/licenses/by/4.0/), which permits unrestricted use, distribution, and reproduction in any medium, provided the original work is properly cited

Abstract

Proteus mirabilis is considered as a third common cause of catheter-associated urinary tract infection, with urease production, the potency of catheter blockage due to the formation of biofilm formation is significantly enhanced. Biofilms are major virulence factors expressed by pathogenic bacteria to resist antibiotics; in this concern the need for providing new alternatives for antibiotics is getting urgent need, This study aimed to explore whether green synthesized zinc oxide nanoparticles (ZnO NPs) can function as an anti-biofilm agent produced by *P.mirabilis*. Bacterial cells were capable of catalyzing the biosynthesis process by producing reductive enzymes. The nanoparticles were synthesized from cell free extract of *P.mirabilis*. Characterization of biosynthesized zinc nanoparticles was carried out to determine the chemical and physical properties of the product using AFM, TEM, FESEM, XRD and UV visible spectrometry. The hexagonal structure was confirmed by XRD, Particle size was marked at 84.45 nm by TEM, FESEM was used to confirm the surface morphology. AFM analysis was used to reveal the roughness and distribution of nanoparticles. UV-visible spectra of the synthesized nanoparticles recorded maximum peak at 287 nm. Zinc nanoparticles showed remarkable biofilm inhibitory effect on clinical isolates of multidrug resistant *Proteus mirabilis*. Strong biofilm producer strains show weak biofilm production After incubation for 24 and 48 hours at 37C° with 32 µg/ml sub - MIC concentration of ZnO nanoparticles. Down regulation changes in *LuxS* expression using Real time PCR technology were detected after treatment with zink nanoparticles of these isolates compared to untreated isolates. From all findings conducted by this study, zinc oxide nanoparticles can function as anti-bacterial agent in concentration dependent manner.

Keywords: Biofilm, Green synthesis, LuxS, Nanoparticles, Zinc oxide.

Introduction

Proteus mirabilis is one of the most frequent links to human disease from pathogenic *Proteus* species. *P. mirabilis* is commonly associated with urinary tract infections (UTIs) in people with structural or functional abnormalities, patients undergoing urinary catheterization can suffer from ascending

infections¹. *Proteus* has been shown the ability to produce biofilms in various situations from aquatic environments to indwelling devices, ureteral stents and urethral catheters. *P. mirabilis* can also produce biofilms on biological surfaces as well as nonliving

surfaces including, glass, polystyrene, silicone, latex².

Bacterial Biofilms are well organized communities with single or multi species enclosed by a defensive polysaccharide matrix containing, extracellular DNA, lipids, and proteins³. The community of biofilm depends on complicated communications, enabling the pathogens to develop resistance against host defense mechanisms, different stress factors and antibiotics⁴. Bacterial biofilms are ubiquitous in clinical settings, since they can increase bacterial resistance up to 1000 folds in comparison to planktonic cells. Subsequently, anticipation measures taking place in hospitals and other clinical settings, nosocomial infections still result in major morbidity and mortality rate⁵. In this emergency situation, researchers are commended to improve new alternatives to traditional antibiotic treatment which can successfully combat multidrug resistance (MDR) and biofilm producing bacteria⁶.

Green synthesis of metal oxide NPs has gained great interest since it is clean, eco-friendly approach and there wide range of applications in biotechnology and medical field⁷. Plant and plant leaf extract is often used as a biological synthesis route ZnO

Materials and Methods

Sample collection: A total of 100 urine samples were collected from patients that have urinary tract infection and resident hospital patients with urine catheters presented to AL Yarmouk teaching hospital in the period from 10/12/2021 to 01/06/2022.

Isolation and identification: *P.mirabilis* was identified primarily by culturing on MacConkey and Blood agar (HiMedia/India) at 37C for 24 h. and confirmed by VITEC 2 system.

Antibiotic susceptibility test:

According to Clinical & Laboratory Standards Institute: CLSI Guidelines 2021, susceptibility test takes place using disk method on Mueller Hinton agar plates. The antibiotics used were (Levofloxacin 5 µg/Disk, Ciprofloxacin 15 µg/Disk, Ampicillin 25µg/Disk, Gentamicin 10 µg/Disk, Cefoxitin 30 µg/Disk, Ticarcilline + Clavulanic acid 85µg/Disk, Piperacillin-Tazobactam 100/10 µg/Disk, Cefepime

nanoparticle displays variable shapes and sizes with minimum surface area that allows them to penetrate microbial cells, therefore, it is considered a powerful antibacterial agent against wide-range of bacterial species⁸.

ZnO NPs are one of the most important nanoparticles of metal oxides; it is a unique and inorganic materials that can be used in several biological applications (anti-bacterial, anti-inflammatory). Several studies described quorum sensing systems as a potential target for antimicrobial agents that limit biofilm formation⁹. Researchers in recent years employ nanotechnology to improve antimicrobials that can target virulence factors without disturbing mammalian cells. Zinc NPs exhibit distinctive properties other than other nanoparticles such as higher solubility, better biofilm penetration and effective drug delivery¹⁰. The anti-Quorum Sensing and the biofilm inhibitory properties of silver nanomaterials have been well recognized¹¹.

This study was aimed to determine the anti-biofilm activity of eco-friendly green synthesized zinc oxide nanoparticles on biofilm production by *P.mirabilis*, changes in *LuxS* expression had been also investigated in this study.

30 µg/Disk, Nitrofurantoin 300 µg/Disk) manufactured by HiMedia (India).

ZnO preparation

Zinc acetate ($Zn(O_2CCH_3)_2$) was used in this research as a precursor.

Bacterial suspension preparation

P. mirabilis were grown in 250 ml of Brain heart broth at 37C for 24 hours in incubator, the bacterial broth then centrifuged and the supernatant were collected and the sediment discarded.

Synthesis of ZnO NPs

ZnO NPs were synthesized by precipitation method, 20g of zinc acetate was added to 200ml of *P. mirabilis* cell free extract at room temperature 37C°, sealed and covered with black plastic bag. After incubation in shaker incubator for 24 h, the mixture was then centrifuged and the precipitate was

collected and washed thrice by deionized water. The nanoparticles were synthesized by the extra cellular route where metal ions get reduced by the action of bacterial reducing enzymes. Nanoparticles formation can be detected by color change, the precipitant is then air dried and kept for further characterization ¹².

Characterization of ZnO NPs

Characterization is essential for understanding nanoparticles properties. The following methods were used to determine NPs characteristics: for determining shapes and sizes, SEM and TEM were used. SEM is used to characterize and visualize surface morphology, particle size distribution, particle/crystal shape, agglomeration of nanoparticles and surface functionalization and in single-particle analysis. TEM uses an electron beam to image a nanoparticle sample, providing much higher resolution than is possible with light-based imaging techniques. Atomic force microscopy (AFM) is used to define height and volume of NPs in 3D vision, UV-visible- (UV-DRS) is used to study the optical property of the samples. (XRD) is a technique used in materials science to determine the crystallographic structure of a material ¹³.

MIC determination:

The estimation of (MIC) was carried out to obtain the minimum concentration of ZnO nanoparticles that inhibits bacterial growth by broth microdilution method using Eppendorf tubes, the bacterial inoculum was prepared in MHB and the concentration was modified to 100 UFC/ μ l. Two fold serial dilutions of ZnO NPS were prepared in 16, 32, 64, 128, 256, 512 μ g/ μ l using MHB in six tubes, the tubes were then incubated for 24 hours at 37° C. Results then achieved by detecting visible growth of bacteria in each tube and sub MIC can then be determined ¹⁴.

Estimation of biofilm formation

Quantitative determination of biofilm formation was determined by a colorimetric microtiter plate assay ¹⁵.

1- Brain heart infusion Broth supplemented with an additional 1% glucose was used for this assay

2-Biofilm inoculums for cultivation was made from bacteria cultivated in broth diluted 1:100 and poured into the well with 200 μ l. The only broth is used in

the negative control wells (200 μ l of BHI supplemented with 1% glucose per well). Each strain was tested in three different ways.

3- Under static conditions, the inoculated plate was covered with a lid and incubated aerobically for 24–30 hours at 35–37°C.

4- The contents of the wells were decanted, and each well was washed three times with 300 μ l of PBS 2.2.5.1. The plates were then drained inverted and fixed with 150 ml methanol.

5- Staining was done with 150 μ l of crystal violet at room temperature for 15 min, then washed and dried at room temperature.

6- For dye re solubilizing, 150 μ l of 95 percent ethanol was added, and the microtiter plate was covered with the lid and left at room temperature for at least 30 min. without shaking.

7- Using a microtiter-plate reader (GloMax/Promega-USA), the optical density (OD) of each well was measured at 630 nm, and the results were as follows:

- $OD \leq OD_c$ = no biofilm producer.
- $OD_c < OD \leq 2 OD_c$ = weak biofilm producer.
- $2 OD_c < OD \leq 4 OD_c$ = moderate biofilm producer;
- $4 OD_c < OD$ = strong biofilm producer.

The cut-off value for the negative control is OD_c , which is defined as three standard deviations (SD), above the mean OD of the negative control: OD_c = average OD of negative control + (3 \times SD of negative control).

Effect of CuO NPs on Biofilm formation

This assay was carried out by 96- well microtiter plate as performed by Punniyakotti., *et al* ¹⁶. tested isolates were cultured in brain heart infusion broth at 37°C for 24h, 100 μ l of bacterial inoculum was attuned to 0.5 McFarland and added to each well, 100 μ l of ZnO suspension were add to each well at the sub-inhibitory concentration then the tubes was incubated at 37C for 48h. Positive control was presented as bacterial culture without Nano formulations while clear broth was considered as

negative control. The contents of each well was discarded after incubation, the microplate was rinsed thrice with sterile saline and dried for 45 min at 60°C. 200 ml of 0.1% of crystal violet were used in staining followed by incubation at room temperature for 15 min; the microplate was rinsed three times with sterile normal saline, Then acetic acid at 30% was added to each well by 200 ml, the optical density (OD) was read at 630 nm for all wells using a microtiter plate reader.

RT-qPCR protocol

The presence of *LuxS* and *rpo* of *P.mirabilis* was determined by employing the thermal cycler to amplify the isolated genomic DNA (Thermo Fisher Scientific, USA). This main step can be separated into two stages, first stage was done by synthesis of cDNA from RNA using specific primer for *LuxS*, *rpo* transcripts and proto script cDNA synthesis kit. This procedure has been performed as detailed in the manufacturing procedure.

The second stage of this protocol was done by taking cDNA samples from tested isolates and controlling at the same run, for each sample there are three PCR tubes, one tube for *LuxS* gene, *rpo* from (macrogen® .Korea). Which is considered a housekeeping gene in this study. The fluorescent power of Syber Green (NEB.UK) is used for quantity estimation. The reaction mix of components with their quantity is mentioned in Table 1 below:

Table 1. Synthesis of cDNA from RNA using primers for *LuxS*, *rpo* transcripts.

Component	Volume
Luna Universal Master Mix	10 ul
Forward primer	1 ul
Reverse primer	1 ul
Template DNA	5 ul
Nuclease-free Water	3 ul
Total volume	20 ul

The difference in cycle thresholds (Ct) and fold changes between the treated groups and the calibrators for each gene were evaluated. The *rpo* values were used to normalize the data using Livak formula¹⁷.

$$\text{Folding} = 2^{-\Delta\Delta C_t}$$

$$\text{Gene expression} = 2^{-\Delta C_t}$$

$$\Delta\Delta C_t = \Delta C_{t \text{ Treated (T)}} - \Delta C_{t \text{ Untreated (C)}}$$

$$\Delta C_t = C_{t \text{ of target gene}} - C_{t \text{ of housekeeping gene}} \dots \text{Untreated}$$

$$\Delta C_t = C_{t \text{ of target gene}} - C_{t \text{ of housekeeping gene}} \dots \text{Treated}$$

PCR tubes were spanned and the liquid were collect (1 minute at 2000g, then the program for Real-Time PCR was setup with indicated thermos cycling protocol. The result was collected and analyzed by Livak formula. With temperatures ranging from 72°C to 95°C at 0.3°C/s, a melting curve was obtained and relative quantitation was used to determine expression levels as shown in Table 2.

Table 2. q RT-PCR program

Step	Temperature (°C)	Minute: Second	Cycles
Reverse transcription (RT).	37	15:00	1
Enzyme activation			
Initial Denaturation	95	10:00	
Denaturation	95	00:15	40
Annealing	50 ^a , 58 ^b , 60 ^c	00:30	
Extension	72	00:30	

Statistical Analysis

All experiments were performed in triplicate and data was expressed as mean and standard deviation. The effect of study variables on biofilm was tested

using the T test. These statistical analyses were done using SPSS version 26 software. The differences were considered significant when P<0.05.

Results and Discussion

Isolation and identification:

A total of sixty four Isolates were confirmed as *P. mirabilis*, the conformation was carried out by VITEK 2 system that considered a reliable identification technique, in addition to swarming on blood agar and colony morphology on MacConkey agar, bull's-eye pattern of swarming is a characteristic phenomenon of *P.mirabilis* that can be seen clearly on solid agar surfaces. Robust swarming bacteria, such as the human opportunistic pathogens *Proteus mirabilis* and *Vibrio parahaemolyticus*, exhibit dramatic phenotypic and behavioral responses upon transition to a swarm-permissible surface. Cells are short in liquid and in low-percentage agar; yet, bacterial cells can elongate up to 40-fold and move as a collective swarm on low-wetness high-percentage agar¹⁸. Swarm motility is hypothesized to be coupled with cell elongation, especially during movement on high-percentage agar, partially because increased cell length would allow for the accommodation of additional flagella on a cell's surface¹⁹. Swarming motility is shown in Fig. 1.



Figure 1. Swarming motility of *P. mirabilis* on blood agar at 37C for 24h. incubation.

Antibiotic susceptibility test

MDR strains screen:

Forty out of sixty four isolates were confirmed as MDR strains After incubation at 37C for 24 hours, All tested isolates were resistant to Piperacillin-

Tazobactam, six isolates only were resistant to levofloxacin, while six isolates were found to be resistant to ciprofloxacin, ampicillin did not inhibit the growth of 15 isolates, gentamicin resistance was found in two strains only, six isolates were recorded as ceftioxin resistant, and 17 isolates were resistant to nitrofurantoin. A ten years study in 2019 shows a growing concern about antibiotic resistance in proteae (Proteae tribe includes the genera *Proteus*, *Morganella* and *Providencia*) Based on the results of the study, Resistance rates to third-generation cephalosporins developed significantly (the indicator during the study was ceftriaxone). Resistance to Ceftriaxone has increased by three times in hospitalized patient samples. Another study carried out in china stated that 25 isolated of 54 *P.mirabilis* were classified as MDR the samples were collected from animals from wild life and humans, this study highlighted that *P. mirabilis* produces AmpC β -lactamases and extended spectrum β -lactamases that makes this bacteria an serious public health risk. *P. mirabilis* uses efflux pump also to resist the main classes of antibiotics²⁰. The antibiotic resistance percentage of given isolates is shown in Table 3.

Table 3. Antibiotic resistance percentage in clinical isolates

Antibiotics	Percentage of resistance
Piperacillin-Tazobactam	100%
levofloxacin	15%
ciprofloxacin	15%
Ampicillin	37.5%
Gentamicin	5 %
Ceftioxin	15%
nitrofurantoin	42.5%

Biosynthesis of Zinc Oxide Nanoparticles:

Zinc oxide nanoparticles were synthesized using cell free extract of *P.mirabilis*. The formation of nanoparticles was indicated by the formation of light yellow to white precipitate. After centrifugation, the precipitate appeared in white color after drying with microwave we obtained shiny white powder. In recent years, an obvious coordination to use bacteria to synthesizes nanomaterials (mainly silver, zinc, gold, and

nanoparticles) with remarkable properties have been observed for the development antimicrobials with in vitro activities against pathogenic bacteria ²¹. Bacteria is easy culturing microorganism with short generation time, these characteristics make bacteria a grate candidate for nanoparticle synthesis as they

have extra cellular reduction enzymes ²². Several types of bacteria such as *E.coli*, *P.fluoresces Serratia sp.*, and *P.stutzeri* approved their ability to reduce certain metal ions and produce nanoparticles ²³. As shown in Fig. 2.

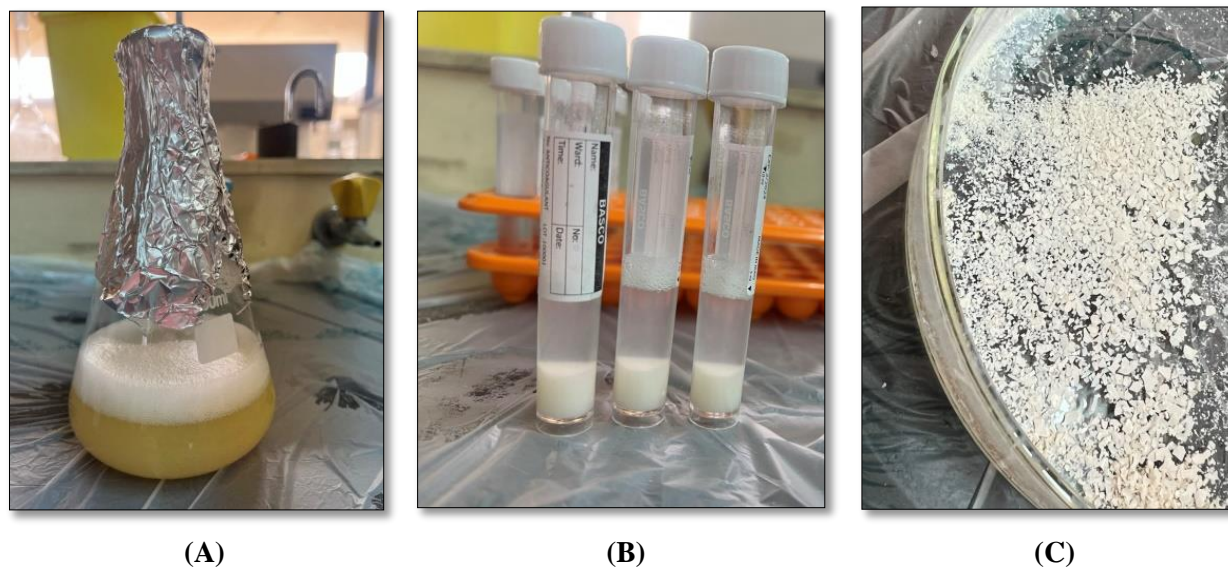


Figure 2. Biosynthesis of zinc nanoparticles
A: Cell free extract with zinc acetate after incubation
B: Sedimentation of nanoparticles after centrifugation
C: zinc oxide nanoparticles powder after drying

Characterization of ZnO NPs

UV-Vis Spectral Analysis

UV-visible spectroscopic analysis was directed to confirm the biogenic synthesis of ZnO NPs. For this typical analysis, the sample was dissolved in deionized water. The results confirmed the formation of freshly prepared biosynthesized ZnO Nps at maximum peak 287 nm. this indicates nanoparticles

in excitation form from ground state to excited state ¹⁹. ZnO shows Narrow size distribution because particles are in Nano scope, thus, a sharp absorption peak can be seen. Zinc oxide nanoparticles are suitable for medical applications like antiseptic ointments and sunscreen protectors as a result of having good absorption in UV region 200-400 nm ²⁴. as shown in Fig. 3

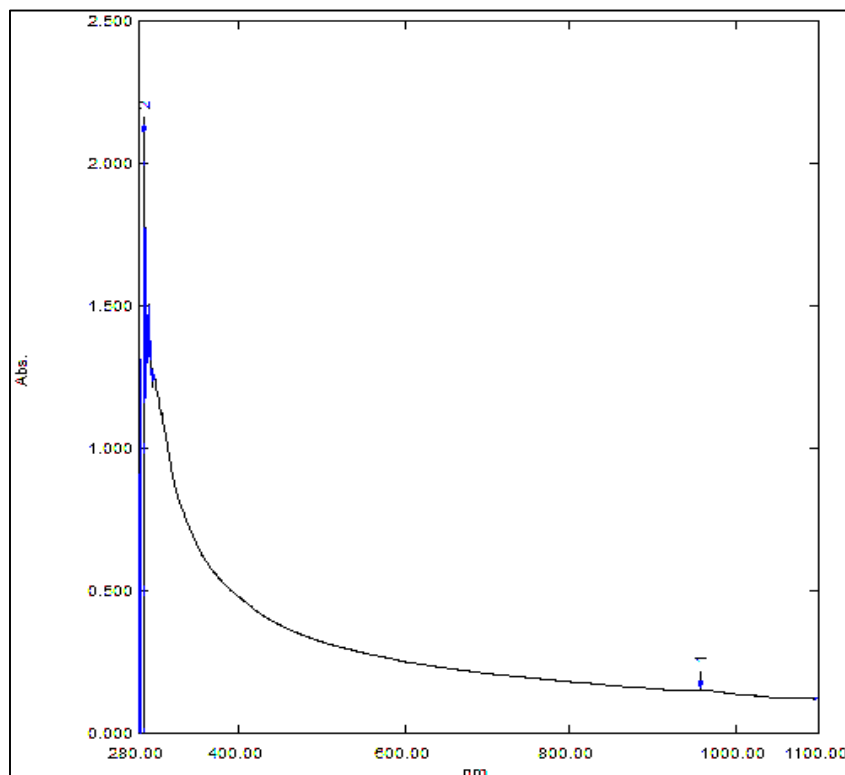
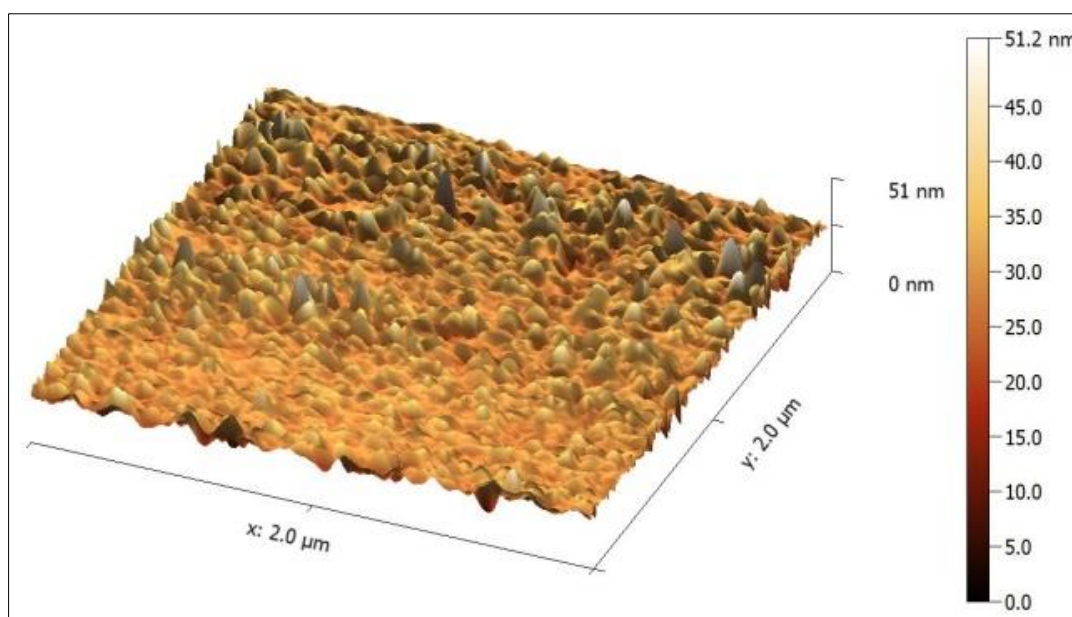


Figure 3. The UV analysis of bio synthesized ZnO NPs

Atomic Force Microscopy (AFM) analysis

AFM analysis of ZnONPs was performed with (CSPM) to identify and characterize distributions of nanoparticles. Estimated grain size and mean square roughness were determined. Portraits three-dimensional profile of ZnO NPs; 3D image of the

ZnO nanoparticles shows that the average grain size is 84.45 nm. Different magnification ranges were conducted to give an insight into the roughness and topography of nanoparticles 2.0 μm and 0.78 μm . As shown in Fig. 4.



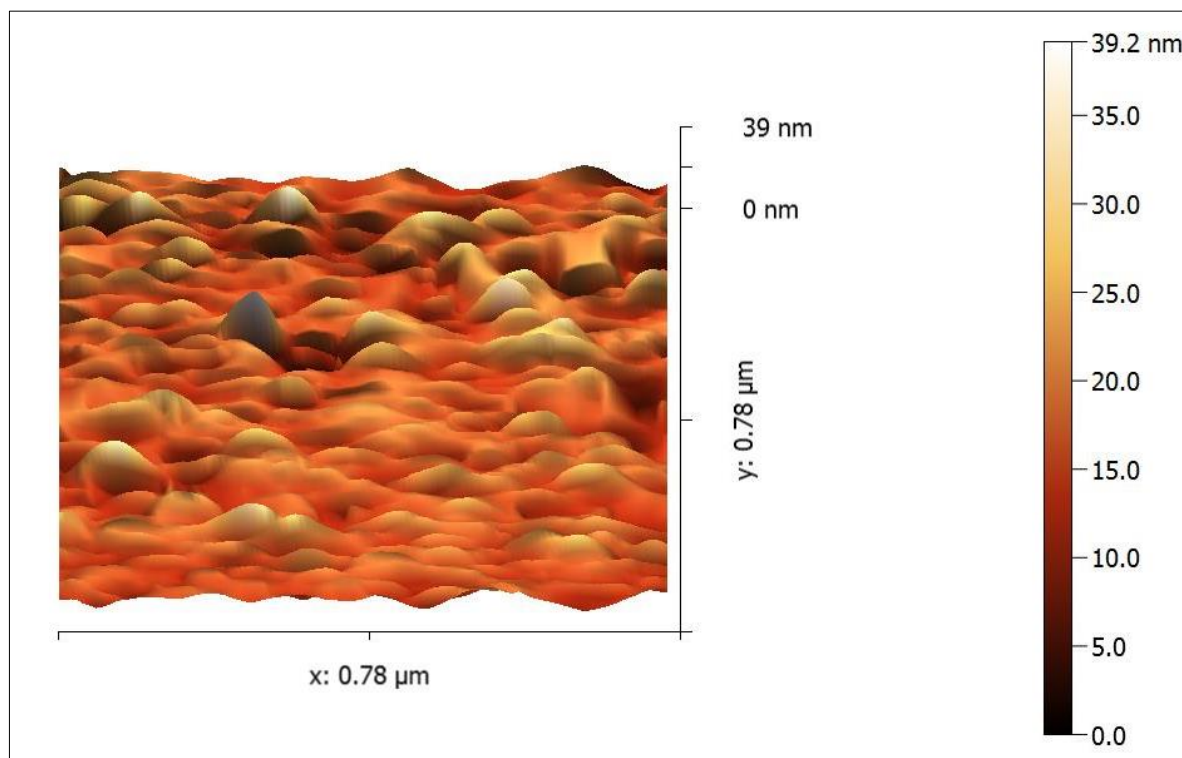


Figure 4. Atomic Force Microscopy analysis of ZnO nanoparticles

Transmission Electron Microscopy analysis (TEM)

The TEM imaging was used to explore the morphology and size of ZnO NPs. The Core structure of the nanoparticles is confirmed by TEM analysis²⁵. TEM images demonstrated the formation of spherical shaped particles with agglomeration in 12.930 kilo pixel magnifications and 300 nm resolution powers. As shown in Fig. 5.

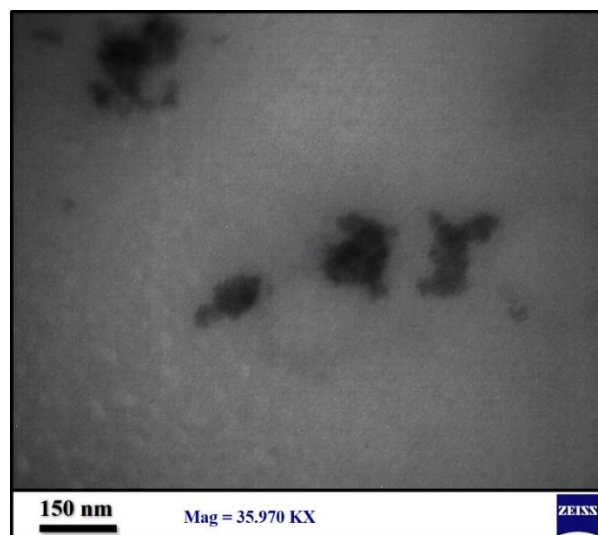
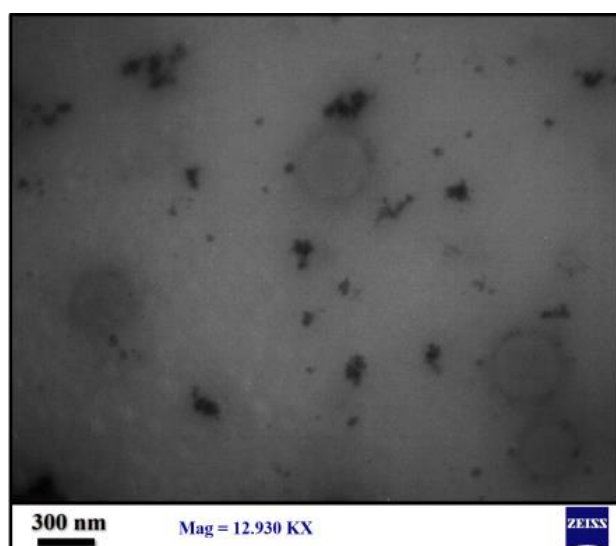


Figure 5. The Transmission Electron Microscopic (TEM) images of ZnO Nps

Field emission Scanning Electron Microscope (FESEM)

SEM analysis was performed to understand the morphology and size as well as the elemental and structural composition of NPs samples. Images show the spherical shape of ZnO NPs at 13000x and 50000x magnification power. SEM images revealed that it was essentially spherical and uniform in

appearance with the diameter ranging from 15 to 19nm. In comparison with EDX-ray, FESEM allows

to determine the presence of different components in the examined model ²⁶. As shown in Fig. 6.

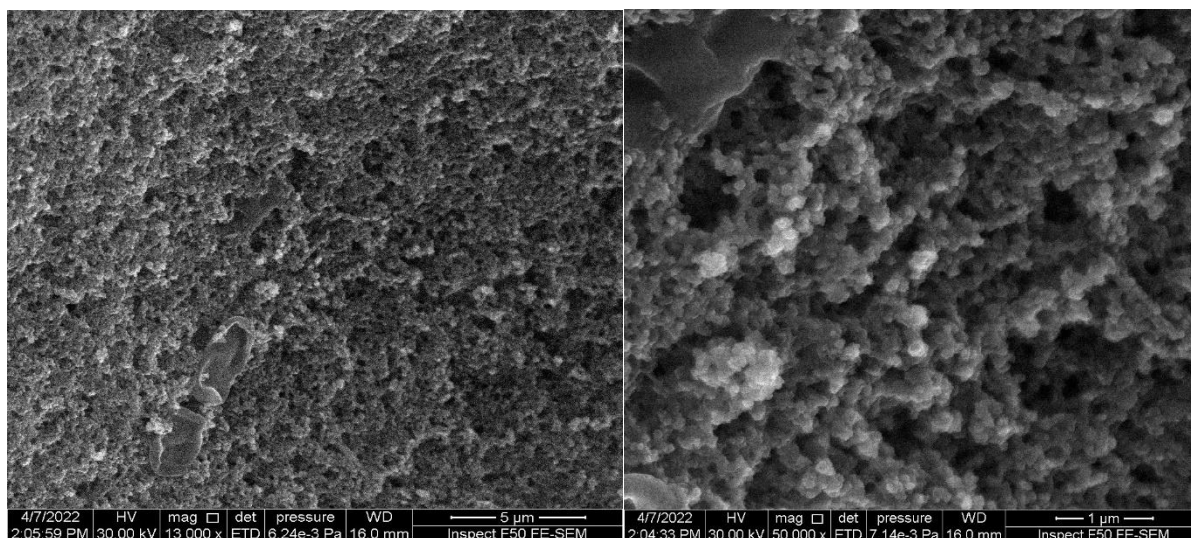


Figure 6. FESEM Images of ZnO Nps

X-ray Diffraction XRD

Spectra of ZnO NPs powder are confirmed by The XRD, the ZnO NPs by revealing 11 prominent peaks corresponding to the diffraction peaks at 2θ values 11.948, 20.241, 24.792, 28.271, 31.458, 45.19, 48.423, 56.242, 63.191, 65.986, 75.068. The formation of zinc oxide NPs by biological materials

is undeniably approved by the XRD pattern and the formation of NPs is also confirmed with resultant ICDD NO: 008,79-2205 and 05-0664. Further, these diffraction peaks of ZnO NPs further also showed hexagonal wurtzite structure the formation of crystalline ZnO NPs also confirmed by the narrow diffraction peak obtained. As shown in Fig. 7.

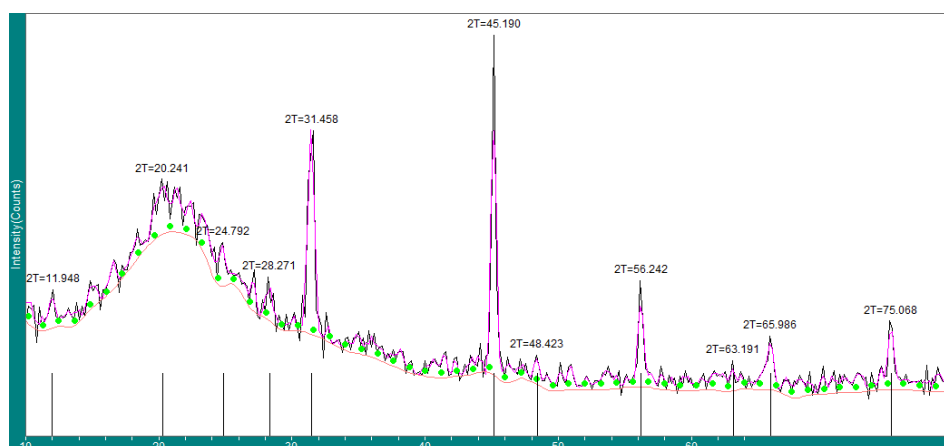


Figure 7. XRD analysis of synergistic ZnO Nps

Determination of biofilm formation before ZnO NPs treatment

A total of 20 MDR isolates were tested for their biofilm production ability using a plastic microtiter plate, nine isolates were recorded as strong biofilm producers as detailed in Table 4. To estimate the effect of ZnO NPs on biofilm production of these

isolates, five strong producers' strains were selected. OD of each well was read at 630 nm using a microtiter plate reader. Fig. 8 shows biofilm production of used clinical isolates.

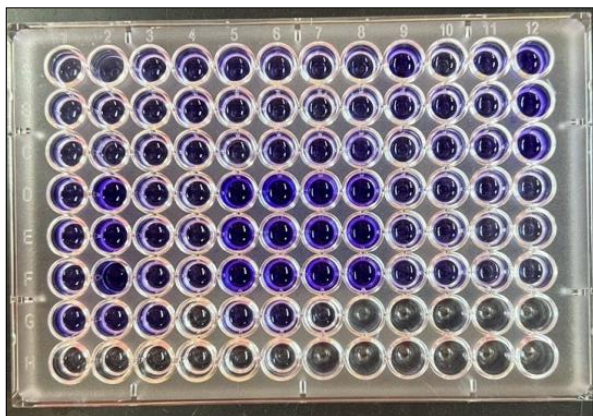


Figure 8. Microtiter plate assay for biofilm production

Determination of biofilm formation after ZnO NPs treatment

Biofilm production was significantly reduced after 48 hours of incubation in 37C with sub MIC of ZnO NPs, OD measurement of the same nine strains of *P.mirabilis* lowered from strong to weak production as detailed in Table 4 and Fig. 9.

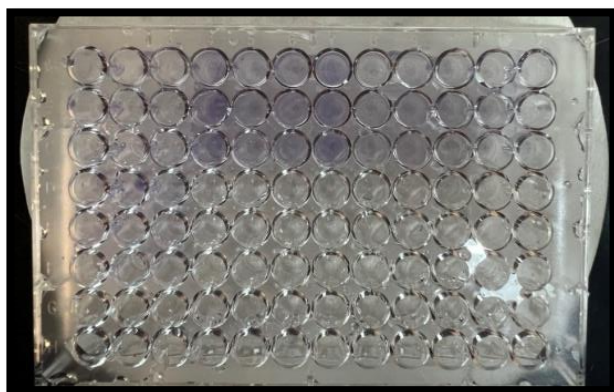


Figure 9. Microtiter plate assay for biofilm production after treatment with ZnO NPs Sub MIC

Table 4. O.D values before and after treatment with biogenic ZnO.

NO. of isolate	O.D treatment	Before	O.D treatment ZnO NPs	after wirh
1.	5.75		1.0	
2.	9.19		1.45	
3.	6.30		1.11	
4.	7.25		1.14	
5.	7.15		1.17	

Antimicrobial action can be explained due to the small particle size of ZnONPs because smaller materials can enter bacterial cell membranes and cause cell damage. Anti-biofilm activity of zinc oxide NPs was previously reported in several studies, one study showed significant decrease in biofilm formation of *pseudomonas aeruginosa* after treatment with zinc oxide NPs in concentration dependent manner²⁷. Biofilm formation is considered a target for different antimicrobial agents such as nanoparticles from different sources, Silver NPs synthesized from Date palm extract against *E. coli* and *K. pneumonia*²⁸. This study also agreed with other studies that approved the Anti biofilm activity against methicillin resistant *S. Aureus*¹⁰. Kouhkan, 2020 displayed that the small size of the NPs could increase the antibacterial effect of these particles due to large surface area that increases their concentration²⁹. Nanoparticles can act on many levels and targets of bacterial components such as eDNA that play a key role in bacterial adhesion, aggregation, biofilm formation and structure, biofilm integrity, in addition to intercellular communication or QS for transfer of genetic information³⁰. Protein inhibition can result in a total destruction of biofilm and planktonic bacterial cells since they are involved in varied functions. Therefore, proteins are one of the important targets in recent antimicrobial therapies³¹. Recent study found that LPS from Gram-negative bacteria like *P. aeruginosa*, *Salmonella enterica* and *E. coli* bind Au nanoparticles, and the binding strength depends on the interaction of LPS with polyelectrolytes. A strong interaction between anionic LPS and cationic NPs was detected by the authors³². Suggesting that electrostatic interactions played a major role in LPS interaction with NPs. This action can be explained by the Reactive Oxygen Species generated by nanoparticles that impose oxidative stress causing bacterial cell destruction.

Studies also found that treatment with nanomaterials induced major reduction of membrane potential signifying it may target membranes of bacterial cells³³.

Gene expression of *LuxS*

LuxS is a transcript of structural operon *luxCDABF* that is responsible for production of autoinducer 2 AI-2 which predominantly participates in cell to cell

signaling in bacteria. The transcription of *luxS* is enhanced when *luxR* is bound to autoinducer. After *luxS* produced, AI-2 cast signals that are used to sense inter species interaction and its own cell density in a multi microbial populations that have essential roles in the regulation of virulence factors³⁴. RT-PCR reveals a major down regulation in *LuxS* expression after exposure to ZnO NPs suspension compared to normal gene expression in bacterial broth with no NPs involved. Fold change in gene expression reveals that *LuxS* was down regulated in response to zinc oxide NPs in three out of five isolates of *P.mirabilis*, the other two isolates were almost not affected.

This result corresponds with the phenotypic changes in biofilm formation in microtiter plate experiment carried out in this study. This finding was accepted by other reports by Rajalakshmi and Sangeetha³⁵. Anti-biofilm activity of metal oxide nanoparticles gained a great interest in last decades, since biofilm is an important virulence factor that enables the bacteria to resist antibiotics³⁶. Several studied approved that these particles have bactericidal and bacteriostatic activity, Khan *et al.* confirms the down regulation effect of ZnO NPs on *las* & *pqs* systems that controls quorum sensing and biofilm production in *P. aeruginosa*³⁷. Other reports estimate the ability of Nano oxides to inhibit QS systems of *S.agalactiae*³⁸. As entailed in Table 5.

Table 5. gene expression changes before and after ZnO NPs

Isolate No.	Ct before treatment with ZnO Nano.			Ct after treatment with ZnO Nano.				Fold Change
	Ct <i>rpo</i>	Ct <i>LuxS</i>	ΔCt	Ct <i>rpo</i>	Ct <i>LuxS</i>	ΔCt	ΔΔCt	
P.1A	16.68	17.36	0.68	18.02	17.45	-0.57	0.84	0.558
P.2B	13.77	11.75	-2.02	11.23	10.75	-0.48	1.54	0.34
P.3C	12.4	10.91	-1.49	14.31	13.25	-1.06	0.43	0.74
P.4D	11.03	11.67	0.64	14.63	14.86	0.23	0.41	1.32
P.5E	10.31	10.47	0.16	10.62	10.69	0.07	-0.09	1.06

Fold change in gene expression reveals that *LuxS* was down regulated in response to Zinc oxide NPs in three out of five isolates of *P.mirabilis*, the other two isolates were almost not affected. This could be due to the development of bacterial resistance mechanisms to nanoparticles, recent studies entailed several possible mechanisms used by bacteria to overcome nanoparticles effect especially by over expression of genes responsible for the production of biofilm components such as exopolysaccharides and development of resistance after many cultures steps³⁹ or up-regulation of efflux pump proteins and molecular interactions (electrostatic interactions)⁴⁰. Zinc generates toxic hydroxyl radicals (OH⁻), that damage cell membranes of Gram-negative and positive bacteria⁴¹. Positively charged metal nanoparticles can create a strong bond with

membranes; this can lead to an increase in their permeability and, therefore, disruption of cell walls, the most important factors determining the interaction with nanoparticles is biofilm maturity and thickness. As shown by Peulen and Wilkinson, EPS is denser in mature biofilms. Hence, the number of pores and the pore sizes are extensively reduced in mature biofilms, making them difficult for nanoparticles to penetrate. Accordingly, thus, the antimicrobial activity of nanoparticles is higher in younger biofilms⁴².

Anti-biofilm activity of metal oxide nanoparticles gained great interest in last decades, since biofilm is an important virulence factor that enables the bacteria to resist antibiotics³⁸. Several studies approved that these particles have bactericidal and bacteriostatic activity, Raheem in 2020 revealed that

ZnO can reduce biofilm formation in *Pseudomonas fluorescens* by tube method⁴³. Another study showed that ZnO nanoparticles acted as powerful antimicrobial agent against *Proteus vulgaris* According to diameter of inhibition Zone⁴⁴. The effect of metal based nanoparticles depends on particle size, morphology and composition. Dispersion, aggregation or agglomeration also plays

a key role in nanoparticles effect. Most studies pointed out the effect of zinc oxide NPs on quorum sensing system on the signal perception and response rather than synthesis of autoinducers. Other reports revealed the effect of polymeric Nano formulations on biofilm cell attachment of *Pseudomonas aeruginosa* (PAO1)^{45 46}.

Conclusion

An alarming situation has been by multi-resistant bacterial strains that have driven the research in the direction of finding novel therapies to combat the infections and diseases associated with bacterial biofilms.

ZnO NPs were successfully synthesized following an in, direct, eco- friendly, low cost, high-yield and green method, ZnO NPs showed exceptional antimicrobial activity against several bacterial strains. Thus, ZnO NPs can be used for external usages as antibacterial agents by coating surfaces on various substrates to prevent biofilm producing microorganisms from attaching and colonizing in indwelling medical devices. In order to modulate the nature of nanoparticle–biofilm interactions are to

make copper oxide nanoparticles are highly selective against one component of the biofilm via bio conjugation techniques. Zinc oxide NPs draped with different chemical moieties have proven to fair better than uncoated nanoparticles in terms of their interactions with the biofilm and antibacterial activity. The application of nanoparticles is increasing nowadays due to their effectiveness in all fields of science. Green synthesized Nano materials that are mostly used in drug delivery and medical approaches have some downsides in using these metal oxides because of their higher toxicity when it is used in higher concentration. All former conclusions highlights that there is an actual need for more investigation in order to use ZnO-NPs as encouraging alternates antibacterial materials.

Authors' Declaration

- Conflicts of Interest: None.
- We hereby confirm that all the Figures and Tables in the manuscript are ours. Furthermore, any Figures and images, that are not ours, have been

- included with the necessary permission for re-publication, which is attached to the manuscript.
- Ethical Clearance: The project was approved by the local ethical committee in University of Baghdad.

Authors' Contribution Statement

The work was carried out by collaboration between all authors N. H. diagnosis the cases and collect the samples and doing the tests, analysis the data and

revisions idea, M. E. edited the manuscript and revision ideas. All authors read and approved the final manuscript.

References

1. Muhammad MH, Idris AL, Fan X, Guo Y, Yu Y, Jin X, et al. Beyond risk: Bacterial biofilms and their regulating approaches. *Front Microbiol.* 2020; 11: 928. <http://dx.doi.org/10.3389/fmicb.2020.00928>.
2. Shokouhfar M, Kermanshahi R-K, Feizabadi M-M, Teimourian S, Safari F. Lactobacillus spp. derived biosurfactants effect on expression of genes involved in *Proteus mirabilis* biofilm formation. *Infect Genet Evol.* 2022; 100(105264): 105264. <http://dx.doi.org/10.1016/j.meegid.2022.105264>.
3. Spirescu VA, Şuhan R, Niculescu AG, Grumezescu V, Negut I, Holban AM, et al. Biofilm-resistant nanocoatings based on zno nanoparticles and linalool. *Nanomaterials.* 2021; 11(10): 2564. <https://doi.org/10.3390/nano11102564>.
4. Balaure PC, Grumezescu AM. Recent advances in surface nanoengineering for biofilm prevention and

- control. Part ii: active, combined active and passive, and smart bacteria-responsive antibiofilm nanocoatings. *Nanomaterials*. 2020; 10(8): 1527. <https://doi.org/10.3390/nano10081527>.
5. Kazemzadeh-Narbat M, Cheng H, Chabok R, Alvarez MM, de la Fuente-Nunez C, Phillips KS, et al. Strategies for antimicrobial peptide coatings on medical devices: a review and regulatory science perspective. *Crit Rev Biotechnol*. 2021; 41(1): 94–120. <https://doi.org/10.1080/07388551.2020.1828810>.
 6. Alwash A. The green synthesise of zinc oxide catalyst using pomegranate peels extract for the photocatalytic degradation of methylene blue dye. *Baghdad Sci J*. 2020; 17(3): 0787–0787. <https://doi.org/10.21123/bsj.2020.17.3.0787>.
 7. Kadhim AA, Salman JAS, Haider AJ, Ibraheem SA, Kadhim H ali. Effect of zinc oxide nanoparticles biosynthesized by *leuconostoc mesenteroides* ssp. *Dextranicum* against bacterial skin infections. In: 2019 12th (DeSE): IEEE; 2019: 755–760. <https://doi.org/10.1109/DeSE.2019.00141>.
 8. Jiang Q, Chen J, Yang C, Yin Y, Yao K. Quorum sensing: a prospective therapeutic target for bacterial diseases. *Biomed Res Int*. 2019; 2019: 1–15. <https://doi.org/10.1155/2019/2015978>.
 9. Wiegand I, Hilpert K, Hancock REW. Agar and broth dilution methods to determine the minimal inhibitory concentration (MIC) of antimicrobial substances. *Nat Protoc*. 2008; 3(2): 163–75. <http://dx.doi.org/10.1038/nprot.2007.521>.
 10. Banerjee S, Vishakha K, Das S, Dutta M, Mukherjee D, Mondal J, et al. Antibacterial, anti-biofilm activity and mechanism of action of pancreatin doped zinc oxide nanoparticles against methicillin resistant *Staphylococcus aureus*. *Colloids Surf B Biointerfaces*. 2020; 190: 110921. <https://doi.org/10.1016/j.colsurfb.2020.110921>.
 11. Husain FM, Khan MS, Ahmad I, Khan RA, Al-Shabib NA, Oves M, et al. Nanomaterials as a novel class of anti-infective agents that attenuate bacterial quorum sensing. In: Ahmad I, Ahmad S, Rumbaugh KP (eds.) *Antibacterial Drug Discovery to Combat MDR*. Springer Singapore; 2019. p. 581–604. https://doi.org/10.1007/978-981-13-9871-1_26.
 12. Ali MdA, Ahmed T, Wu W, Hossain A, Hafeez R, Islam Masum MdM, et al. Advancements in plant and microbe-based synthesis of metallic nanoparticles and their antimicrobial activity against plant pathogens. *Nanomaterials*. 2020; 10(6): 1146. <https://doi.org/10.3390/nano10061146>.
 13. Phang YK, Aminuzzaman M, Akhtaruzzaman Md, Muhammad G, Ogawa S, Watanabe A, et al. Green synthesis and characterization of *cuo* nanoparticles derived from papaya peel extract for the photocatalytic degradation of palm oil mill effluent(Pome). *Sustainability*. 2021; 13(2): 796. <https://doi.org/10.3390/su13020796>.
 14. Jaffar N, Miyazaki T, Maeda T. Biofilm formation of periodontal pathogens on hydroxyapatite surfaces: Implications for periodontium damage: Biofilm Formation of Periodontal Pathogens on Hydroxyapatite Surfaces. *J Biomed Mater Res A*. 2016; 104(11): 2873–2880. <https://doi.org/10.1002/jbm.a.35827>.
 15. Gajdács M, Urbán E. Comparative epidemiology and resistance trends of proteae in urinary tract infections of inpatients and outpatients: a 10-year retrospective study. *Antibiotics*. 2019; 8(3): 91. <https://doi.org/10.3390/antibiotics8030091>.
 16. Punniyakotti P, Panneerselvam P, Perumal D, Aruliah R, Angaiah S. Anti-bacterial and anti-biofilm properties of green synthesized copper nanoparticles from *Cardiospermum halicacabum* leaf extract. *Bioprocess Biosyst Eng*. 2020; 43(9): 1649–1657. <https://doi.org/10.1007/s00449-020-02357-x>.
 17. Passat DNF. Local Study of blaCTX-M genes detection in *Proteus* spp. by using PCR technique. *Iraqi J Sci*. 2016; 57(2c): 1371–1376. <https://ijs.uobaghdad.edu.iq/index.php/eijs/article/view/7107>
 18. Kang Q, Wang X, Zhao J, Liu Z, Ji F, Chang H, et al. Multidrug-resistant *Proteus mirabilis* isolates carrying bla OXA-1 and bla NDM-1 from wildlife in China: increasing public health risk. *Integr Zool*. 2021; 16(6): 798–809. <https://doi.org/10.1111/1749-4877.12510>.
 19. Little K, Austerman J, Zheng J, Gibbs KA. Cell shape and population migration are distinct steps of *Proteus mirabilis* swarming that are decoupled on high-percentage agar. *J Bacteriol*. 2019; 201(11): e00726-18. <http://dx.doi.org/10.1128/JB.00726-18>.
 20. Tuson HH, Copeland MF, Carey S, Sacotte R, Weibel DB. Flagellum density regulates *Proteus mirabilis* swarmer cell motility in viscous environments. *J Bacteriol*. 2013; 195(2): 368–77. <http://dx.doi.org/10.1128/JB.01537-12>.
 21. Grasso G, Zane D, Dragone R. Microbial nanotechnology: challenges and prospects for green biocatalytic synthesis of nanoscale materials for sensoristic and biomedical applications. *Nanomaterials*. 2019; 10(1): 11. <https://doi.org/10.3390/nano10010011>.
 22. Kouhkan M, Ahangar P, Babaganjeh LA, Allahyari-Devin M. Biosynthesis of copper oxide nanoparticles using *lactobacillus casei* subsp. *Casei* and its anticancer and antibacterial activities. *Curr Nanosci*. 2020; 16(1): 101–111. <https://doi.org/10.2174/1573413715666190318155801>.

23. Janani B, Syed A, Raju LL, Al-Harhi HF, Thomas AM, Das A, et al. Synthesis of carbon stabilized zinc oxide nanoparticles and evaluation of its photocatalytic, antibacterial and anti-biofilm activities. *J Inorg Organomet Polym Mater*. 2020; 30(6): 2279–2288. <https://doi.org/10.1007/s10904-019-01404-9>.
24. Duffy LL, Osmond-McLeod MJ, Judy J, King T. Investigation into the antibacterial activity of silver, zinc oxide and copper oxide nanoparticles against poultry-relevant isolates of *Salmonella* and *Campylobacter*. *Food Control*. 2018; 92: 293–300. <https://doi.org/10.1016/j.foodcont.2018.05.008>.
25. AL-Asady ZM, AL-Hamdani AH, Hussein MA. Study the optical and morphology properties of zinc oxide nanoparticles. In: Baghdad, Iraq; AIP Conf Proc. 2020. 2213(1) p. 020061. <https://doi.org/10.1063/5.0000259>.
26. Kassinger SJ, van Hoek ML. Biofilm architecture: An emerging synthetic biology target. *Synth Syst Biotechnol* .2020; 5(1): 1–10. <http://dx.doi.org/10.1016/j.synbio.2020.01.001>.
27. Khan MohdF, Husain FM, Zia Q, Ahmad E, Jamal A, Alaidarous M, et al. Anti-quorum sensing and anti-biofilm activity of zinc oxide nanospikes. *ACS Omega*. 2020; 5(50): 32203–32215. <https://doi.org/10.1021/acsomega.0c03634>
28. Siddiqi KS, ur Rahman A, Tajuddin, Husen A. Properties of zinc oxide nanoparticles and their activity against microbes. *Nanoscale Res Lett*. 2018; 13(1): 141. <https://doi.org/10.1186/s11671-018-2532-3>.
29. Shah S, Gaikwad S, Nagar S, Kulshrestha S, Vaidya V, Nawani N, et al. Biofilm inhibition and anti-quorum sensing activity of phytosynthesized silver nanoparticles against the nosocomial pathogen *Pseudomonas aeruginosa*. *Biofouling* .2019; 35(1): 34–49. <http://dx.doi.org/10.1080/08927014.2018.1563686>.
30. Abadeer NS, Fülöp G, Chen S, Käll M, Murphy CJ. Interactions of bacterial lipopolysaccharides with gold nanorod surfaces investigated by refractometric sensing. *ACS Appl Mater Interfaces* .2015; 7(44): 24915–25. <http://dx.doi.org/10.1021/acsami.5b08440>.
31. Hasson SO, kadhem Salman SA, Hassan SF, Abbas SM. Antimicrobial effect of eco- friendly silver nanoparticles synthesis by iraqi date palm (*Phoenix dactylifera*) on gram-negative biofilm-forming bacteria. *Baghdad Sci J*. 2021; 18(4): 1149–1156. <https://doi.org/10.21123/bsj.2021.18.4.1149>
32. Bondarenko OM, Sihtmäe M, Kuzmičiova J, Ragelienė L, Kahru A, Daugelavičius R. Plasma membrane is the target of rapid antibacterial action of silver nanoparticles in *Escherichia coli* and *Pseudomonas aeruginosa*. *Int J Nanomedicine*. 2018; 13: 6779–6790. <https://doi.org/10.2147/IJN.S177163>.
33. Hussein EI, Al-Batayneh K, Masadeh MM, Dahadhah FW, Al Zoubi MS, Aljabali AA, et al. Assessment of pathogenic potential, virulent genes profile, and antibiotic susceptibility of *proteus mirabilis* from urinary tract infection. *Int J Microbiol*. 2020; 2020: 1–5. <https://doi.org/10.1155/2020/1231807>.
34. Rajalakshmi, Sangeetha, Udhaya. Effect of antifungal drugs against candida isolates from diabetic women with vaginitis. *J Infect Dis Ther*. 2017; 05(04): 1-5. <http://dx.doi.org/10.4172/2332-0877.1000331>.
35. Jabin Mishu N, Sm S, Hm K, Nabonee MA, zannat dola N, haque A. Association between biofilm formation and virulence genes expression and antibiotic resistance pattern in *proteus mirabilis*, isolated from patients of dhaka medical college hospital. *Arch Clin Biomed Res*. 2022; 06(03): 418–434. <https://doi.org/10.26502/acbr.50170257>.
36. Badawy MSEM, Riad OKM, Taher FA, Zaki SA. Chitosan and chitosan-zinc oxide nanocomposite inhibit expression of LasI and RhII genes and quorum sensing dependent virulence factors of *Pseudomonas aeruginosa*. *Int J Biol Macromol*. 2020; 149: 1109–1117. <https://doi.org/10.1016/j.ijbiomac.2020.02.019>.
37. Abdul-Hamza HK, Mohammed GJ. Anti-quorum sensing effect of streptococcus agalatiaceae by Zinc Oxide, Copper Oxide, and Titanium Oxide nanoparticles. *J Phys : Conf Ser* . 2021; 1999(1): 012031. <https://doi.org/10.1088/1742-6596/1999/1/012031>.
38. Cai X, Liu X, Jiang J, Gao M, Wang W, Zheng H, et al. Molecular mechanisms, characterization methods, and utilities of nanoparticle biotransformation in nanosafety assessments. *Small*. 2020;1 6(36): 1907663. <https://doi.org/10.1002/sml.201907663>.
39. Joshi ASPAMI. Interactions of gold and silver nanoparticles with bacterial biofilms: Molecular interactions behind inhibition and resistance. *Int J Mol Sci*.. 2020; 21(20). <https://doi.org/10.3390/ijms21207658>.
40. Sistemática D, Gabriela SS, Daniela FR, Helia BT. Zinc nanoparticles as potential antimicrobial agent in disinfecting root canals. *Odontostomat*. 2016; 10(3): 547–54.
41. Peulen T-O, Wilkinson KJ. Diffusion of nanoparticles in a biofilm. *Environ Sci Technol*. 2011; 45(8): 3367–73. <http://dx.doi.org/10.1021/es103450g>.
42. Raheem H, Yasser H. Silver Nanoparticles as Antibacterial Action against *Pseudomonas Fluorescens* Isolated from Burn Infection. *Ann Romanian Soc Cell Biol*. 2021; 25(4): 12578–83. <https://www.annalsofrscb.ro/index.php/journal/article/view/4189>.

43. Chaudhary A, Kumar N, Kumar R, Salar RK. Antimicrobial activity of zinc oxide nanoparticles synthesized from Aloe vera peel extract. SN Appl Sci . 2019; 1: 136. <https://dx.doi.org/10.1007/s42452-018-0144-2>.
44. Gómez-Gómez B, Arregui L, Serrano S, Santos A, Pérez-Corona T, Madrid Y. Unravelling mechanisms of bacterial quorum sensing disruption by metal-based nanoparticles. Sci Total Environ. 2019; 696: 133869. <https://doi.org/10.1016/j.scitotenv.2019.133869>.
45. Alavi M, Li L, Nokhodchi A. Metal, metal oxide and polymeric nanoformulations for the inhibition of bacterial quorum sensing. Drug Discov Today. 2022; 28(1): 103392. <https://doi.org/10.1016/j.drudis.2022.103392>.
46. Rashid AE, Ahmed ME, Hamid MK. Evaluation of Antibacterial and Cytotoxicity Properties of Zinc Oxide Nanoparticles Synthesized by Precipitation Method against Methicillin-resistant *Staphylococcus aureus*. Int J Drug Deliv Technol. 2022; 12(3): 985-989. <https://doi.org/10.25258/ijddt.12.3.11>.

تأثير دقائق اوكسيد الزنك النانوية المصنعة بايولوجياً على النمط الظاهري والجيني للغشاء الحيوي لبكتريا *Proteus mirabilis*

نور حمزة فائق، ميس عماد أحمد

قسم علوم الحياة، كلية العلوم، جامعة بغداد، بغداد، العراق.

الخلاصة

تصنف بكتريا *Proteus mirabilis* ككائنات مسببة لالتهاب المجاري البولية المصاحب لتركيب أنابيب القسطرة البولية. تعد الاغشية الحيوية من عوامل الضراوة التي تستعملها البكتريا لمقاومة المضادات الحيوية وفي ضل تطور مقاومة البكتريا للمضادات الحيوية. صار لزاماً على العلماء والباحثين في مجال الاحياء المجهرية إيجاد بدائل ذات كفاءة عالية قادرة على اختراق جدار الخلية البكتيرية وبالتالي قتلها. في السنوات الاخيرة، اكتسبت دقائق النانو المصنعة بايولوجيا والصديقة للبيئة اهتماماً كبيراً من قبل الباحثين لأمتلاكها خصائص مميزة كصغر حجمها المتناهي واشكالها المختلفة يمكنهم من استعمالها كمواد مضادة للبكتيريا في مختلف المجالات الطبية والصحية. تهدف هذه الدراسة الى التحري عن قدرة دقائق اوكسيد النحاس النانوية المصنعة بايولوجيا على تثبيط تكوين الغشاء الحيوي المنتج من قبل بكتيريا *Proteus mirabilis*. أنتجت هذه الدقائق بأستعمال راشح بكتيري يحتوي على الانزيمات المختزلة لملح النحاس واستخدمت عدة تقنيات لتحديد الصفات الفيزيائية المظهرية لدقائق النانو المنتجة حيث استخدمت تقنية XRD لتأكيد التركيب خماسي الشكل لهذه الدقائق , بينما استعملت تقنية TEM لتحديد قطر الجزيئات المنتجة بمعدل 84.45 نانومتر. اما FESEM فقد تم استخدامه لتحديد الصفات الخارجية لسطح جزيئات النانو المنتجة , تم تأكيد النتائج بأستخدام تقنية AFM للكشف عن توزيع و وعورة جزيئات النانو. اما UV فقد سجلت الاقصى امتصاصية على الطول الموجي 287nm. تم التحري في هذه الدراسة عن فعالية دقائق اوكسيد النحاس النانوية في منع تكون الغشاء الحيوي حيث أستعمل مستحلب دقائق اوكسيد النحاس النانوي بالتركيز تحت القاتل 32 µg/ml . سجلت نتائج هذه الدراسة انخفاضاً ملحوظاً في انتاج الغشاء الحيوي للبكتريا المنتجة له حيث سجلت العزلات ذات الانتاجية العالية للغشاء الحيوي ضعفاً في الانتاج بعد معاملتها بالتركيز المستعمل من دقائق اوكسيد النحاس النانوية. جاء تأثير هذه الدقائق على كل من النمط الظاهري والتعبير الجيني لجين *LuxS* المسؤول عن تكوين الغشاء الحيوي بأستخدام تقنية rtPCR حيث سجلت الدراسة انخفاضاً في التعبير الجيني لهذا الجين بعد معاملة سلالات البكتريا قيد الدراسة بدقائق اوكسيد النحاس النانوية مقارنةً بالعزلات غير المعاملة. من خلال نتائج هذه التجربة يمكن التوصل الى امكانية اعتماد دقائق اوكسيد الزنك النانوية كعامل مضاد للبكتيريا عن استخدامه بالتركيز المناسب.

الكلمات المفتاحية: الاغشية الحيوية ، تخليق أخضر ، لوكس ، جزيئات نانوية ، أكسيد الزنك.